DISCRETE FRACTURE SIMULATION OF WELL CAPTURE ZONES IN BEDROCK

Abigail J. Easton, Bernard H. Kueper
Department of Civil Engineering, Queen's University, Kingston, Ontario

ABSTRACT

A Discrete Fracture Network (DFN) model was created using FracMan® to evaluate hydraulic capture of an existing pump and treat system at a former PCB transfer facility in Smithville, Ontario. A sensitivity analysis of the DFN model to varying model input parameters was carried out to demonstrate to site investigators what aspects of the fracture network are most influential in determining the aerial and vertical extent of capture. Two separate three level factorial designs were used to carry out the sensitivity analysis. Analysis of Variance tables were utilized to interpret the factorial design analyses. Of the input parameters studied, mean bedding plane fracture (BPF) aperture, mean vertical fracture (VF) aperture, BPF and VF P32 have the greatest impact on capture zone area and need to be better characterized than BPF size and VF termination % in order to predict capture.

RÉSUMÉ

Un modèle de Réseau de Fracture Discrète (RFD) a été créé avec FracMan afin d'évaluer la capture hydraulique d'un système de pompe et traitement existant à des anciennes installations de transfert de PCB à Smithville, ON. Une analyse de sensibilité du modèle RFD aux paramètres des données variables a été exécuté afin de démontrer aux investigateurs les aspects du réseau de fracture les plus influents en déterminant la mesure verticale et aérienne de capture. Deux plans factoriels à trois niveaux ont été employés afin d'exécuter l'analyse de susceptibilité. Une analyse des tableaux de variance a été employé afin d'interpréter les analyses des plans factoriels. Parmi les paramètres des données étudiés, l'ouverture moyenne de BPF, l'ouverture moyenne de VF, BPF et VF P32 ont l'impact le plus grand sur la zone de capture, et doivent être mieux caractérisés que la taille de BPF et le pourcentage de terminaison de VF afin de prédire la capture.

1. INTRODUCTION

A lot of focus has been placed on groundwater research in recent years because of the fact that groundwater contamination by light and dense non-aqueous phase liquids (LNAPLS and DNAPLS, respectively) has been identified as a serious problem warranting immediate attention. In fractured rock, DNAPL moves though a network of fracture pathways and comes to rest as both pooled and residual NAPL (Kueper and McWhorter, 1991). It is often important to assess the area of capture of an extraction well system at a contaminated site. Capture zones define the area around a pumping/extraction well from which water is captured by the well for a specified time period or at steady-state conditions.

The objective of this research was to create a Discrete Fracture Network (DFN) model to evaluate hydraulic capture of an existing pump-and-treat system in Smithville, Ontario and to conduct a sensitivity analysis of the model output to varying model input parameter values to demonstrate to site investigators what aspects of the fracture network are most influential in determining the aerial and vertical extent of capture.

2. STUDY SITE

The Discrete Fracture Network (DFN) model created using FracMan® was used to evaluate hydraulic capture of an existing pump and treat system at a former PCB transfer facility (CWML site) on the northern perimeter of the town of Smithville in southern Ontario. The CWML site was operated as a hazardous waste transfer station between 1978 and 1985. It is estimated that 434,000 L of liquid waste were handled during that time. The majority of the wastes transferred were polychlorinated biphenyls (PCBs) and other related DNAPLs. A site map showing the DNAPL source zone and selected monitoring wells and boreholes is shown in Figure 1.

3. DISCRETE FRACTURE NETWORK MODEL

The program FracMan®, developed by Golder Associates Inc. (Seattle, WA), was used to generate fracture networks. FracMan® is a well-recognized, commercially available fracture generation model that is used for hydrogeologic and geotechnical applications. The input to FracMan® is primarily in the form of statistical

distributions; these were based on data present in the Smithville Site database.

Once a fracture network was generated using FracWorksXP and the finite element mesh was generated using MeshMaster, the program MAFIC was used to simulate groundwater flow through the network.

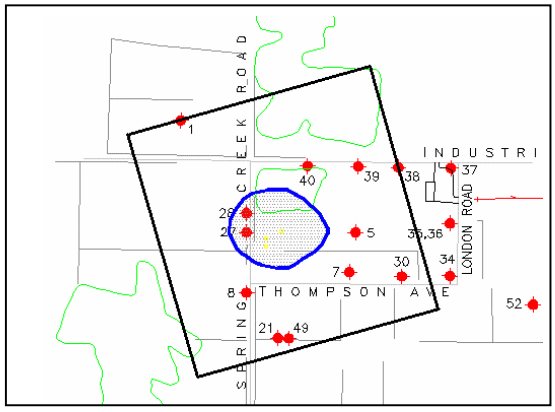

Figure 1 – Site Map

3.1 MODEL INPUT

The Lockport formation in the Smithville region is made up of four members. From ground surface downwards these are the Eramosa member, the Vinemont member, the Gasport member and the Goat Island member. Because the conceptual model for the site assumes that significant quantities of DNAPL are not present below the Eramosa Member, it is deemed not essential that capture be assessed at those depths. As a result, the solution domain only included the Eramosa member.

To generate a DFN in FracMan® the following input parameters need to be specified: aperture, transmissivity, storativity, orientation, geometric model, termination %, fracture size, and P32 (related to fracture spacing). In this study, fracture intensity was specified using P32, which allows specification of the area of fractures per unit volume of rock. In FracWorksXP, fracture size is represented in terms of a mean equivalent radius.

3.1.1 FRACTURE SPACING AND INTENSITY

The bedding plane fracture (BPF) spacing specified in the model, which represents the Eramosa member, is 0.39 m. This corresponds to a P32 value of 2.56 m^{-1}. The bedding plane fracture spacing is assumed to be spatially uniform for all simulations.

A vertical fracture (VF) spacing of 30 m was used to generate fracture networks. This corresponds to a P32 value of 0.033 m^{-1}. Vertical fracture spacing is assumed to be spatially uniform in each simulation.

3.1.2 FRACTURE SIZE

A mean bedding plane fracture size of 100 m was used when generating the discrete fracture network realizations. Bedding plane fracture size was assumed to follow a normal distribution with a mean of 100 m and a standard deviation of 33 m. The vertical fracture size was assumed to follow a normal distribution with a mean of 15 m and a standard deviation of 3 m.

3.1.3 TERMINATION %

In this study a constant termination percentage of 40 % was assumed for each of the vertical fracture sets. Because the bedding plane fracture set is the first set generated in the model, termination % has no impact on this fracture set.

3.1.4 ORIENTATION

The formation at the study site is near flat-lying dolostone that dips to the south with a mild gradient of 1 % - 2 %. In the FracMan® model, bedding plane fractures were modeled as horizontal fractures. The three major vertical fracture sets identified in the Eramosa were generated in the discrete facture network model. The orientations of the strike of the three sets generated are 100º, 065º and 000º.

3.1.5 HYDROGEOLOGIC PARAMETERS

For each of the three hydrogeologic properties that FracWorksXP assigns to each generated fracture, namely transmissivity, storativity, and fracture aperture, the respective mean value and distributional form were specified. In this study, values of fracture transmissivity and fracture aperture are required for steady-state groundwater flow simulations.

Fracture transmissivity and aperture distributions were determined through analysis of 0.1 m hydraulic test data (Novakowski et al., 2000) for boreholes 37c, 54a, 54d, 56 and 64. In this procedure, it is assumed that the tested interval of interest contained one conductive horizontal fracture. Of the available distributional forms, the exponential distribution was found to fit the data best. The mean aperture was found to be 1.0e-03 m. Vertical fracture aperture was assumed to follow an exponential distribution with a mean of 1.07e-04 m for each of the three sets.

4. FRACMAN SOLUTION DOMAIN

The FracMan® solution domain encompasses the DNAPL source zone and the eight extraction wells. The domain spans a maximum of 600 m in the north-south direction, 600 m in the east-west direction, and extends 13 m below the ground surface. The Eramosa formation in the modelling region is 13 m thick. Extraction well pumping rates and locations for the eight extraction wells are shown in Table 1 and Figure 2, respectively.

Table 1 – Extraction Well Pumping Rates

Extraction Well	Pumping Rate (m^3/s)
RWS2	1.123e-05
RWS3	8.137e-05
RWS5	2.430e-04
RWS6	2.731e-05
RWS7	1.956e-05
PEW1	7.650e-05
PEW2	7.650e-05
PEW3	7.650e-05

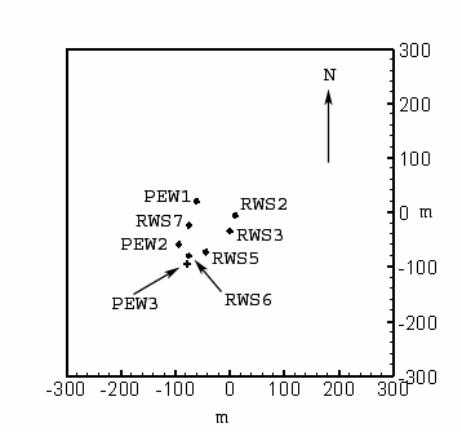

Figure 2 – Extraction Well Locations in FracMan® Domain

4.1 GENERATION OF MODEL DOMAIN

Stochastic fracture patterns are generated in the FracMan® software component FracWorksXP. One horizontal bedding plane fracture set and three vertical fracture sets were generated. The Center Points method was used for fracture generation. Fractures were therefore generated with their centers inside the generation region. The Enhanced Baecher geometric model was selected. As such, fracture centers were located uniformly in space according to a random Poisson Process.

FracMan® supports Monte Carlo analyses, which allows different stochastically similar realizations of the model to be generated. Each realization of the fracture network was combined with the same boundary condition file (.SAB file) containing all necessary boundary conditions, pumping well locations and extraction rates and all necessary input data required by MAFIC to solve for flow and carry out particle tracking.

4.2 BOUNDARY CONDITIONS

Boundary conditions for the FracMan® discrete fracture model have been determined based on the results of the calibrated Frac3dvs model completed by Queen's University for the Smithville site (Queen's, 2001a). The top boundary was assigned a constant flux of 0.14 m/yr, the side boundaries were assigned no flow boundary conditions, the north and south boundaries were assigned constant head boundaries determined from the calibrated Frac3dvs model of 184.76 m and 183.84 m, respectively. The bottom boundary was assigned a constant head ranging linearly from 184.76 m at the northern edge to 183.84 m at the southern edge of the domain.

4.3 FINITE ELEMENT MESH GENERATION

For each of the discrete fracture networks generated in FracWorksXP, the finite element mesh was created using MeshMaster, a component of the FracMan® software package. In order to generate the finite element mesh, two files are specified, the boundary condition file (.SAB) described in detail above, and the fracture (.FAB) file created in FracWorksXP.

After the initial finite element mesh is created, the mesh is refined to ensure a more detailed and accurate mesh formation. Because fracture transmissivity assigned to each fracture in the discrete fracture network is not related to the specified aperture via the cubic law, fracture transmissivity data was post-processed in EDMESH to ensure that the cubic law was obeyed.

4.4 FLOW AND PARTICLE TRACKING

After the finite element mesh is created for each of the discrete fracture networks generated in FracWorksXP, groundwater flow and particle tracking are solved in MAFIC. MAFIC requires the (.MAF) file created by MeshMaster or a (.MFT) file created by EDMESH.

For this study, MAFIC was used to simulate steady-state flow through each of the generated three dimensional discrete fracture networks. MAFIC uses a Galerkin Finite element solution to solve the equation for flow and transport.

A convective particle tracking approach is used to simulate solute transport in MAFIC. The particle tracking approach was implemented in order to track particles in a forward direction to the extraction wells in the model, and to ultimately discretize capture zones. Backward particle tracking is not supported in the current version of MAFIC.

A total of 8,000 particles were released in each model domain. An arbitrary particle mass was specified with lateral and transverse dispersion both set to zero. 4,000 particles were released on the top of the domain and 4,000 particles were released on the high constant head boundary of each DFN realization.

5. MODEL CALIBRATION

A minimum aperture value of 50 μm was used in the analysis. This procedure is justified by the fact that the smaller aperture fractures will not be as influential with respect to groundwater flow as the larger aperture fractures.

5.1 HORIZONTAL BULK K

In order to compare the value of bulk K (mean: 6.19E-04 m/s, variance: 2.2E-05 m/s) reported in Novakowski et al. (2000) to the bulk K calculated from the FracMan® model, the following analysis was carried out. The FracMan® domain was generated in FracWorksXP using the input statistics for the four fracture sets in the Eramosa member. No-flow boundary conditions were placed along the top, bottom and side faces of the DFN model domain and constant head boundary conditions were placed on the upgradient and downgradient faces. The north boundary was assigned a constant head value of 184.76 m and the south boundary was assigned a constant head value of 183.84 m. Multiple statistically similar discrete fracture networks were generated in FracWorksXP using the built in Monte Carlo function. After solving for flow and transport in MAFIC for each discrete fracture network realization, the horizontal bulk K was calculated according to Darcy's Law.

The FracMan® model input parameter values were adjusted until both the measured and modeled bulk K matched. The base case parameters derived by this process are shown in Table 2. The mean horizontal fracture aperture arrived at through analysis of constant head hydraulic testing was maintained. Figure 3 shows a graph of average horizontal bulk K versus the number of model runs. The graph shows that as the number of realizations increases, average bulk K approaches a constant number and the relative percent error between successive average measurements becomes smaller. The average modelled horizontal bulk K is 6.55e-04 m/s. This is very close to the measured horizontal bulk K of 6.19e-04 m/s for the Eramosa member.

Table 2 – Base Case Parameter Values

Parameter	BPF Value	VF Value
No. of Fracture Sets	1	3
Geometric Model	Enhanced Baecher	Enhanced Baecher
Fracture Shape	Circular	Circular
P32 (m^{-1})	2.56	0.033
Fracture Size		
Distribution	Normal	Normal
Mean, Stdev. (m)	100, 33	15, 3
Aperture		
Distribution	Exponential	Exponential
Mean (m)	1.00e-03	1.07e-04
Storativity	0	0
Orientation (trend, plunge)	000, 90	100, 0 (Set 1)
		065, 00 (Set 2)
		000, 00 (Set 3)

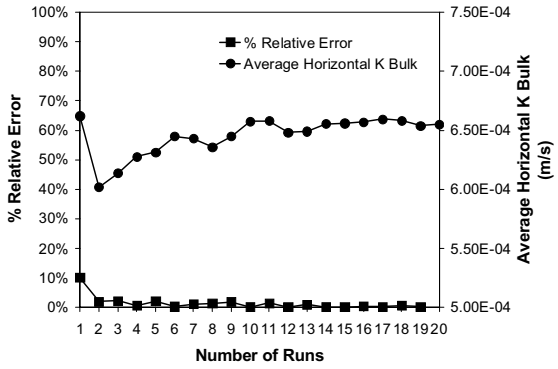

Figure 3 - Average horizontal bulk K and % relative error vs. number of model runs

5.2 VERTICAL BULK K

The vertical bulk K was also calculated from the discrete fracture network model. No flow boundary conditions were placed along the four sides of the three dimensional rectangular domain and constant head boundary conditions were placed on the top and bottom faces. The top boundary was assigned a constant head value of 184.76 m and the bottom boundary was assigned a constant head value of 183.84 m.

After solving for flow and transport in MAFIC, the vertical bulk K was calculated according to Darcy's law. Figure 4 shows a graph of average vertical bulk K versus the number of model runs. The average modelled vertical bulk K is 2.12e-06 m/s, which is two orders of magnitude less than the horizontal value and deemed to be representative of site conditions.

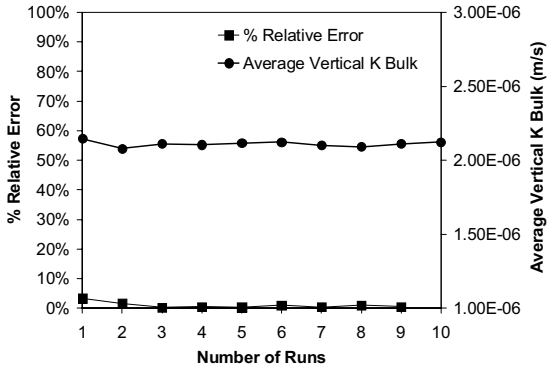

Figure 4 - Average vertical bulk K and % relative error vs. number of model runs

5.3 MAFIC CALIBRATION CHECK

To check the calibration of the base case MAFIC flow solution, modeled water levels were compared to measured water levels in monitoring wells 17S9, 18, 23, 25S7, 26S9, 28S9, 33D16, 33S12, 42S11, 42S8, 44S11, 6S11, 66-6, 66-7, 67-7, 7S17, 8D15, 9D16. Monitoring wells located within the FracMan® solution domain with

screened lengths less than 3 m were chosen for the MAFIC calibration. Multiple base case DFNs were generated in FracWorksXP utilizing the built in Monte Carlo function and combined with a boundary condition file (.SAB) containing information pertaining to the monitoring wells.

A plot of measured vs. modeled heads is shown in Figure 5. The figure shows that the majority of measured vs. modeled hydraulic head values fall within the +1 m and -1 m residuals. However, there are two wells (33S12 and 42S8) that show head values outside of this residual range. These wells are shallow wells that possibly have leaky casings accounting for the higher measured water levels.

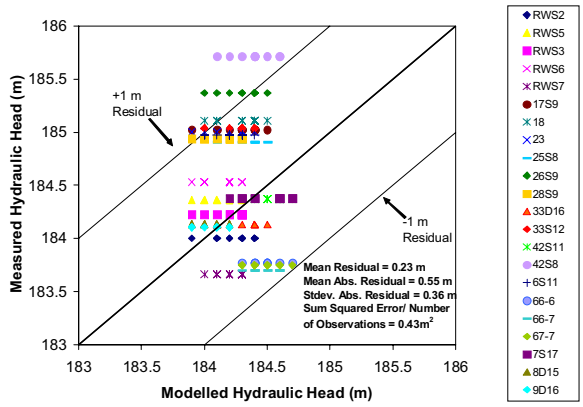

Figure 5 – Measured vs. modeled hydraulic heads

6. SENSITIVITY ANALYSIS

Four parameters, P32 (intensity), termination %, mean fracture aperture, and mean fracture size (equivalent radius) were selected for the sensitivity analysis. Fracture orientation for each of the 4 fracture sets was assumed to be constant given data from the Smithville database and hence was not considered in the sensitivity analysis. Fracture transmissivity is related to aperture via the cubic law, and hence by including aperture in the sensitivity analysis, transmissivity is studied as well. The geometric model selected for this study, as mentioned previously, is the Enhanced Baecher Model. The geometric model was kept the same for all model runs in the factorial design analysis.

6.1 FULL THREE LEVEL FACTORIAL DESIGN

In this study in which it is necessary to quantify the effect of various factors on area and depth of capture, a full three level factorial (3^3) experimental design was used. Two separate factorial designs were conducted; the first evaluated the effect of changing bedding plane fracture (BPF) parameters P32, mean aperture and mean fracture size on area and depth of capture keeping vertical fracture (VF) properties at the base case values. The second factorial design evaluated the effect of changing vertical fracture parameters P32, mean aperture and termination % on area and depth of capture keeping bedding plane fracture properties at the base case values.

The factors and their levels are listed in Table 3. The intermediate level for both the bedding plane fracture and the vertical fracture factorial designs are the base case parameter values determined from the model calibration exercise. The low and high values were chosen around the intermediate base case value and were thought to be reasonable for the parameters in question.

Each of the three vertical fracture sets in the model is assumed to have the same parameter values with the exception of orientation. Therefore, vertical fracture parameters are lumped into one set representative of all sets. The experimental setup for the bedding plane fracture factorial design is shown in Table 4 and the experimental setup for the vertical fracture factorial design is shown in Table 5. The base case simulations are designated by BPF_14 and VF_14.

The design of each setup consisted of 27 experiments with replicates ranging in number from 6 to 11 for which capture zone area (m^2) was measured using a planimeter. The area of each capture zone was measured three times and the average taken in order to ensure accurate measurement.

The results of the factorial design were analyzed by the effects model via an analysis of variance and regression analysis. The first six run results of area and depth of capture for each experiment were used when calculating the ANOVA. However, because there is no stipulation on the number of observations or run results that can be used to fit a regression model, all capture zone area and depth of capture results were used when fitting the least-squares regression model. Only the results of the ANOVA are presented in this paper.

Table 3 - BPF and VF Factorial Design Factors and Levels

	Level		
Factor	**Low**	**Intermediate**	**High**
BPF			
P32 (m^{-1})	1.02	2.56	3.58
Fracture Size (mean, Stdv.) (m)	80, 33	100, 33	140, 33
Mean Aperture (m)	4.64e-04	1.00e-03	2.16e-03
VF			
P32 (m^{-1})	0.013	0.033	0.04
Termination %	20	40	60
Mean Aperture (m)	4.96e-05	1.07e-04	2.30e-04

7 RESULTS

7.1 GENERAL RESULTS

For both the bedding plane fracture and vertical fracture factorial designs, the capture zones are non-uniform and particles follow complex pathways in the discrete fracture network. There is considerable variability in the shape of

capture zones within and between different experiments in the factorial designs. Figures 6 and 7 show the capture zone area and depth of capture

Table 4 - BPF Full 3^3 Factorial Design Setup

		P32 (m^{-1})		
Aperture (m)	Fracture Size (m)	1.02	2.56	3.58
4.640E-04	80	BPF_1	BPF_10	BPF_19
	100	BPF_2	BPF_11	BPF_20
	140	BPF_3	BPF_12	BPF_21
1.000E-03	80	BPF_4	BPF_13	BPF_22
	100	BPF_5	BPF_14	BPF_23
	140	BPF_6	BPF_15	BPF_24
2.155E-03	80	BPF_7	BPF_16	BPF_25
	100	BPF_8	BPF_17	BPF_26
	140	BPF_9	BPF_18	BPF_27

Table 5 – VF Full 3^3 Factorial Design Setup

		P32 (m^{-1})		
Aperture (m)	Termination %	0.013	0.033	0.4
4.960E-05	20	VF_1	VF_10	VF_19
	40	VF_2	VF_11	VF_20
	60	VF_3	VF_12	VF_21
1.07E-04	20	VF_4	VF_13	VF_22
	40	VF_5	VF_14	VF_23
	60	VF_6	VF_15	VF_24
2.3 E-04	20	VF_7	VF_16	VF_25
	40	VF_8	VF_17	VF_26
	60	VF_9	VF_18	VF_27

for two runs in the base case ensemble, which corresponds to simulation 14 in both the BPF (BPF_14) and VF (VF_14) factorial design analyses. Base Case average capture zone area and average depth of capture and % relative error graphs are shown in Figures 8 and 9, respectively.

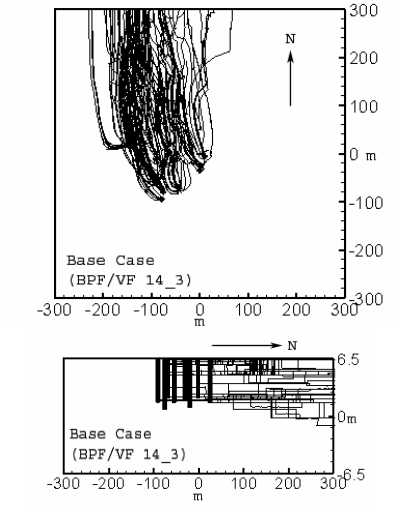

Figure 6 – Base Case (BPF 14_3 and VF 14_3) area and depth of capture figures

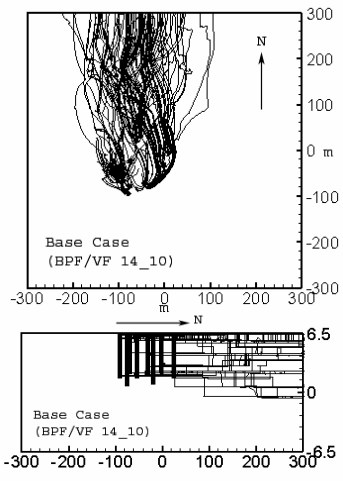

Figure 7– Base Case (BPF 14_10 and VF 14_10) area and depth of capture figures

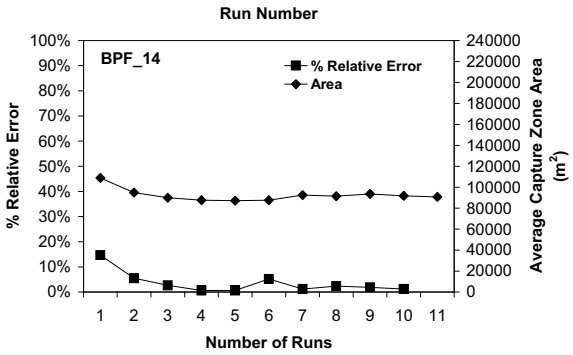

Figure 8 – Base Case average capture zone area and % relative error graph

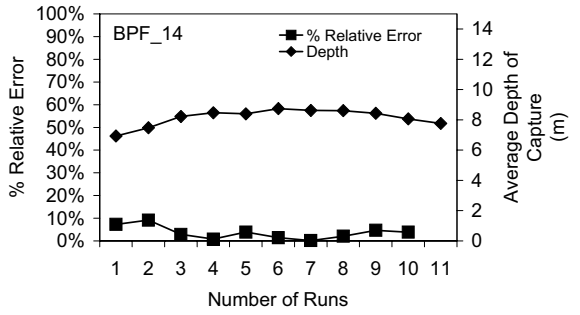

Figure 9 – Base Case average depth of capture and % relative error graph

7.2 ANOVA RESULTS

An Analysis of Variance (ANOVA) was carried out on the log-transformed BPF and VF capture zone area,

respectively, as well as the BPF and VF depth of capture, respectively. Results of the Analysis of Variance for both the BPF and VF factorial designs are shown in Tables 6 to 9.

Table 6 – BPF Factorial Design Area of Capture ANOVA Results

COMPONENT	% OF VAR.	F_o	$F_{0.01}$	$F_{0.05}$
Main Effects	**42.24**			
A (aperture)	4.53	9.53	4.61	3.00
S (size)	0.23	0.48	4.61	3.00
P (P32)	37.48	78.85	4.61	3.00
1st Interactions	**16.91**			
SA	2.99	3.14	3.32	2.37
SP	3.67	3.86	3.32	2.37
AP	10.25	10.78	3.32	2.37
2nd Interactions	**8.76**			
ASP	8.76	4.61	2.51	1.94

The main effects of the BPF factorial design account for 42.2 % of the overall variability in mean capture zone area for all simulations in the factorial design. 4.5 % is due to the mean BPF aperture, 0.23 % is due to the mean BPF size, and 37.5 % is due to BPF P32. First interactions account for 16.9 % of the overall variability in mean capture zone area in the BPF factorial design. 10.3 % is due to the interaction between mean BPF aperture and BPF P32, 3.7 % is due to the interaction between mean BPF size and BPF P32, and 3.0 % is due to the interaction between mean BPF aperture and mean BPF size. Second interaction effects, the interaction between all three parameters studied, account for 8.8 % of the overall variability in mean capture zone area.

Table 7 – VF Factorial Design Area of Capture ANOVA Results

COMPONENT	% OF VAR.	Fo	$F_{0.01}$	$F_{0.05}$
Main Effects	**69.39**			
A (aperture)	65.53	178.01	4.61	3
T (termination %)	0.34	0.93	4.61	3
P (P32)	3.52	9.56	4.61	3
1st Interactions	**4.39**			
TA	0.71	0.96	3.32	2.37
TP	0.74	1.01	3.32	2.37
AP	2.94	3.99	3.32	2.35
2nd Interactions	**1.38**			
FTP	1.38	0.94	2.51	1.94

The main effects of the VF factorial design account for 69.4% of the overall variability in mean capture zone area for all simulations in the factorial design. 65.5 % is due to the mean VF aperture, 0.34 % is due to termination %, and 3.5% is due to VF P32. First order interaction effects account for 4.4 % of the overall variability in mean capture zone area for the VF factorial design. 0.74 % is due to the interaction between VF P32 and VF termination %, 2.9 % is due to the interaction between VF P32 and mean VF aperture, and 0.71 % is due to the interaction between mean VF aperture and VF termination %. Second order effects account of 1.4 % of the overall variability in capture zone area.

Table 8 – BPF Factorial Design Depth of Capture ANOVA Results

COMPONENT	% OF VAR.	Fo	$F_{0.01}$	$F_{0.05}$
Main Effects	**38.06**			
A (aperture)	23.96	32.30	4.61	3
S (size)	0.55	0.75	4.61	3
P (P32)	13.54	18.26	4.61	3
1st Interactions	**11.42**			
SA	1.96	1.32	3.32	2.37
SP	2.16	1.46	3.32	2.37
AP	7.30	4.92	3.32	2.37
2nd Interactions	**0.45**			
ASP	0.45	0.15	2.51	1.94

The main effects of the BPF depth of capture factorial design account for 38.1 % of the overall variability in mean depth of capture for all simulations in the factorial design. 24.0 % is due to mean BPF aperture, 13.5 % is due to BPF P32 and 0.55 % is due to mean BPF size. First interactions account for 11.4 % of the overall variability in depth of capture in the BPF factorial design. 7.3 % is due to the interaction between mean BPF aperture and BPF P32, 2.2 % is due to the interaction between mean BPF size and BPF P32, and 2.0 % is due to the interaction between mean BPF aperture and mean BPF size. Second interaction effects account for 0.45 % of the overall variability in depth of capture.

Table 9 – VF Factorial Design Depth of Capture ANOVA Results

COMPONENT	% OF VAR.	Fo	$F_{0.01}$	$F_{0.05}$
Main Effects	**3.85**			
A (aperture)	2.36	1.99	4.61	3.00
T (termination%)	0.34	0.29	4.61	3.00
P (P32)	1.16	0.97	4.61	3.00
1st Interactions	**15.26**			
TA	3.08	1.30	3.32	2.37
TP	3.16	1.33	3.32	2.37
AP	9.01	3.79	3.32	2.37
2nd Interactions	**0.75**			
ATP	0.75	0.16	2.51	1.94

The main effects of the vertical fracture depth of capture factorial design account for 3.9 % of the overall variability in depth of capture for all simulations in the factorial design. 2.4 % is due to mean VF fracture aperture, 1.2 % is due to VF P32 and 0.34 % is due to VF termination %. First interactions account for 15.3 % of the overall variability in mean depth of capture in the vertical fracture

factorial design. 9.0 % is due to the interaction between mean VF aperture and VF P32, 3.2 % is due to the interaction between VF termination % and VF P32, and 3.1 % is due to the interaction between mean VF aperture and VF termination %. Second interaction effects account for 0.75 % of the overall variability in depth of capture.

8. DISCUSSION

If BPF spacing (i.e., P32) remains constant and mean BPF aperture increases, the bulk K of the fractured rock mass increases. For constant head boundary conditions, the flow through the rock mass therefore increases. As a result, there is less drawdown at the extraction wells for a constant pumping rate and particles further away from the wells are not captured. This accounts for an overall decrease in mean capture zone area as mean BPF aperture increases. Similarly, if mean BPF aperture is held constant and mean BPF spacing decreases, the bulk K of the rock mass increases and there is an overall decrease in mean capture zone area as BPF P32 increases.

As the mean BPF size increases in FracMan®, the equivalent radius of a circle with similar dimensions increases. As a result, as mean BPF size increases, the length and width of the fractures increases. While it may be expected that increasing fracture size should lead to an increase in bulk K and a corresponding decrease in capture area, this is not observed in the current study because the fracture network is highly connected at all three levels of the factorial design (i.e., compared to many other settings, this is a highly fractured rock mass).

As the termination % increases, the vertical fractures become shorter and there is less vertical interconnection in the discrete fracture network. As a result, the horizontal to vertical anisotropy in conductivity increases, and mean capture zone area increases slightly.

9. CONCLUSIONS

With respect to the first factorial design, the effects of mean BPF aperture and BPF P32 were found to significantly affect area and depth of capture, respectively, and accounted for the greatest percentage of variance in mean area and mean depth of capture for all simulations. In general, as mean BPF aperture and BPF P32 increase, the area and depth of capture, respectively, decrease. Mean BPF size accounted for only a small percentage of the overall variance in area and depth of capture and did not significantly affect the mean area and depth of capture. The interaction effects between BPF size and mean BPF aperture and between mean BPF size and BPF P32, respectively, were found to significantly affect capture zone area. The interaction effect between BPF P32 and mean BPF aperture was also found to significantly affect both area and depth of capture.

With respect to the second factorial design, mean VF aperture and VF P32 were found to significantly affect capture zone area and accounted for the greatest percentage of variance in mean capture zone area for all simulations. Termination % only accounted for a small percentage of the overall variance in mean area of capture and did not significantly affect the mean area of capture. In general, as mean VF aperture and VF P32 increase the area and depth of capture, respectively, decrease. Neither VF P32, mean VF aperture, nor VF termination % was found to significantly affect depth of capture. However, the interaction effect between VF P32 and mean VF aperture was found to significantly affect the depth of capture and accounted for the greatest percentage of variance in mean depth of capture for all simulations. The interaction effect between VF P32 and mean VF aperture was also found to significantly affect capture zone area.

The mean BPF aperture, mean VF aperture, BPF P32 (related to fracture spacing) and VF P32 have a significant effect on mean area and depth of capture. As a result, these parameters have a greater effect on the area and depth of capture compared to mean BPF size and VF termination %.

10. REFERENCES

Kueper, B.H. and McWhorter, D.B., 1991. The behavior of dense, non-aqueous phase liquids in fractured clay and rock. Journal of Ground Water, Vol. 29, No. 5, pp. 716-728.

Novakowski, K., Lapcevic, P., Bickerton, G., Voralek, J., Zanini, L., and Talbot, C. 2000. The Development of a Conceptual Model for Contaminant Transport in the Dolostone Underlying Smithville, Ontario.

Queen's University, 2001a. Technical Memorandum, Step 7, Task 7.2, Numerical Model Calibration. Department of Civil Engineering, Queen's University, Kingston, ON.